NASA TECHNICAL MEMORANDUM

NASA TM X-73585

NASA TM X-73585

FERROGRAPHIC ANALYSIS OF WEAR DEBRIS GENERATED IN A SLIDING ELASTOHYDRODYNAMIC CONTACT

by William R. Jones, Jr., H. S. Nagaraj, and Ward O. Winer
Lewis Research Center
Cleveland, Ohio 44135

TECHNICAL PAPER to be presented at the
Annual Meeting of the American Society of Lubrication Engineers
Montreal, Canada, May 9-12, 1977

FERROGRAPHIC ANALYSIS OF WEAR DEBRIS GENERATED IN A SLIDING ELASTOHYDRODYNAMIC CONTACT

by William R. Jones, Jr.
National Aeronautics and Space Administration
Lewis Research Center
Cleveland, Ohio 44135

and

H. S. Nagaraj and Ward O. Winer
Georgia Institute of Technology
School of Mechanical Engineering
Atlanta, Georgia 30332

E-8925

ABSTRACT

The Ferrograph has been used to analyze wear debris generated in a sliding elastohydrodynamic contact. The amount of wear debris correlates well with the ratio of film thickness to composite surface roughness (Λ ratio). Essentially all of the generated wear particles were of the normal rubbing wear type.

INTRODUCTION

Recently, a new instrument, the Ferrograph, has been developed which is capable of magnetically precipitating wear debris from a lubricant onto a glass slide to yield a Ferrogram (1 to 3). The precipitated particles usually range in size from approximately 0.02 to a few micrometers and are arranged according to size on the substrate. The density of the deposit on the substrate may be measured optically, and individual particles may be observed with a unique bichromatic microscope, the Ferroscope.

Elastohydrodynamic lubrication (EHD) refers to the condition of elastically deformed surfaces separated by very thin lubricant films (typically 0.5 to 20 μm thick) (4). Surface separation is achieved by the generation

STAR Category 27

of high hydrodynamic pressures due to the rapid increase of lubricant viscosity with increasing pressures. All highly loaded sliding or rolling machine elements with concentrated contact geometries operate in an EHD or partial EHD regime. Ideally, a complete surface separation is effected. However, under conditions of decreasing speed, increasing load, decreasing viscosity or existence of starvation conditions, surface asperity interactions may occur. As lubricant films become thinner, one may proceed through the following regimes: EHD, partial EHD, boundary, and eventually catastrophic failure.

The objective of this investigation was to use the Ferrograph to determine the total amount of wear debris and the wear particle types generated by a sliding EHD contact as the film thickness was gradually decreased and asperity interactions began to occur.

Three series of test balls (AISI 52100 steel) were used having surface roughness of 0.011, 0.076, and 0.38 μm Ra, respectively. Experimental conditions included a sliding speed of 1.08 meters per second, a range of loads from 8.9 to 522 newtons (maximum Hertz stress range, 0.52 to 2.03 GN/m^2), and a test duration of 25 minutes. Tests were conducted at room temperature.

EXPERIMENTAL APPARATUS AND TECHNIQUE

EHD Apparatus

The EHD apparatus (fig. 1) used in this study has been previously reported (5 to 8). The sliding EHD contact is formed using a 31.8-mm diameter chrome steel (AISI 52100) ball rotating and loaded against a sapphire flat (1.6 mm thick). The infrared radiation at this contact is measured with an infrared radiometric detector having a spot size resolution of 38 μm with a 15× objective. The temperature of the oil reservoir was monitored with a

thermocouple as a function of test time. The oil was not recirculated in these experiments in order to eliminate particle contamination from the recirculation system. A total lubricant charge of 5×10^{-5} cubic meter (50 ml) was used.

Chromium steel balls of three different roughness values were used. The Ra values were 0.011, 0.076, and 0.38 μm and will be referred to as smooth (S), medium rough (MR), and rough (R), respectively. These balls were finished by a standard grinding process and did not have any preferred orientation of the surface pattern. Representative surface profile traces for the three balls and the sapphire flat appear in Fig. 2. Tests will be referred to as S-1, MR-1, R-1, etc., corresponding to the ball roughness and load. Experimental conditions for each test are summarized in Table I.

Film thicknesses were determined optically at the contact center for the smooth ball for each test condition. These values were also used for the medium rough and rough ball series. This was necessary because the interference fringes used to measure film thickness disappear as the roughness increases.

The technique for measuring ball surface temperature has been described earlier (6 and 7). Ball surface temperature measurements were made only at the contact center for the smooth and medium rough balls. The center is easy to locate and the maximum temperature occurs near this location. With the rough ball, the maximum temperature was measured in the contact, whether or not it occurs at the contact center. The disappearance of the interference fringes made it impossible to locate the contact center with the rough ball.

The fluid used in this study is a naphthenic mineral oil containing no additives. It has been designated N1 in previous studies. A complete

description of this fluid appears in appendix A of Ref. 5. A summary of fluid properties appears in Table II.

EHD Apparatus Cleaning Procedure

All oil contacting parts were washed with acetone, dried, and rinsed with distilled water. Then all parts were washed with a dilute acid solution. This solution was prepared by adding 10 drops of concentrated nitric acid and 10 drops of concentrated hydrochloric acid to 5×10^{-5} cubic meter (50 ml) of distilled water. This solution dissolved any metallic debris left from the previous test. The parts were then rinsed with distilled water, a dilute sodium bicarbonate solution, distilled water again, and finally with 95 percent ethanol.

Ferrograph

The Ferrograph (1 to 3) is a commercial instrument used to magnetically precipitate wear particles from a used oil onto a specially prepared glass slide. A mixture of 3×10^{-6} cubic meter (3 ml) of used oil and 1×10^{-6} cubic meter (1 ml) of solvent is prepared. This mixture is then slowly pumped over the slide as shown in Fig. 3. A wash and drying cycle follows which removes residual oil and permanently attaches the particles to the slide. The resulting slide with its associated particles is called a Ferrogram.

The amount of wear debris on a Ferrogram can be determined by measuring the optical density of the deposit at various positions along the slide. In this way, a composite Ferrogram density can be determined for each set of conditions.

Ferrogram slides are approximately 60 mm in length. As shown in Fig. 3, the oil sample first contacts the slide at a position 55 or 56 mm from one end. This area is designated as the entry position. In principle, the

larger wear particles will appear in this region. As the oil traverses the slide there is a gradual gradation in particle size. The smaller particles will then appear in the exit region which is about 10 mm from the end of the slide.

Optical density measurements were made on each Ferrogram at several different locations: entry, 54, 50, 40, 30, 20, and 10 mm. In addition a composite or representative density was determined by averaging the several different readings. A density reading of less than 1 percent was treated as a zero. Optical density measurements for all tests appear in table III.

RESULTS AND DISCUSSION

Ferrogram Results

Photomicrographs of the Ferrogram entry region for each of the tests with the smooth, medium rough, and rough ball series appear in Figs. 4 to 6, respectively. The general trend of increasing wear particle density with increasing load (or decreasing film thickness) is evident in most cases. Occasionally, nonmetallic debris or large oxide flakes, unrelated to the wear process, were observed which caused some high optical density readings. An example of this interference is shown in Fig. 4(b) for the S2 test. In fact, many of the density readings in the smooth series were caused, in part, by this type of debris.

Often pile-ups of both metallic and nonmetallic debris occur at the entry position. Since this makes it difficult to assess the wear level, an alternate procedure is to examine the debris at a location some distance from the entry. Typically this is the 54-mm position. Micrographs taken at this location for all tests appear in Figs. 7 to 9. Again, the trend of the increasing amounts of wear debris with increasing load in both the medium rough and rough ball series is obvious. However, most of the particles present at the

54-mm position in the smooth series are not wear related. These particles are transparent and nonmetallic.

Wear as a Function of Λ Ratio

A convenient parameter for predicting the degree of surface interactions is the ratio of the central film thickness to the composite surface roughness. This dimensionless parameter Λ is mathematically defined as:

$$\Lambda = \frac{h_0}{\left(\sigma_1^2 + \sigma_2^2\right)^{1/2}} \qquad [1]$$

where h_0 is the central film thickness and σ_1 and σ_2 are the Ra surface roughnesses of the two contacting surfaces. In this study, the two surfaces were the sapphire disk and steel ball. Since bath temperature was changing during the tests (and thus h_0) an average $\Lambda(\Lambda_{avg})$ was calculated for each test and appears in Table I.

A plot of composite Ferrogram density for each test as a function of Λ_{avg} appears in Fig. 10. The large and very rapid increase in particle density at low Λ values is evident. The transition to the high wear regime occurs as the Λ ratio approaches 1. This is in agreement with the findings of other investigators. Tallian (9) has shown that the onset of surface distress occurs at a Λ value of about 1.5. Czichos (10) reports that the change from a full EHD film to continuous asperity contact occurs as Λ decreases from 2.5 to 0.7. In Fig. 10, at Λ values greater than 1, a composite particle density of between 1 and 2 percent is observed. Since a full film should be present at these higher Λ ratios, little wear should take place. Therefore, these density readings represent the background or contaminant particle density for this set of experiments.

As shown in Table I, there was an overlap of Λ values in each test

series. There were four sets of tests that yield similar average Λ ratios. These were: S3-MR1, S4-S5-MR2, MR3-R1, and MR4-R2. One would expect the generation of a similar amount of debris under these similar test conditions. The composite Ferrogram densities for these four sets of experiments appear in Fig. 11 and a good correlation is observed.

Wear Particle Morphology

Microscopic examination of the wear debris generated during these studies yielded the following information. Essentially, all of the metallic wear particles, regardless of the initial surface roughness, were of the "normal rubbing wear" variety. That is, they were composed of small asymmetric thin (metallic) flakes. These flakes were typically less than 10 μm in major dimension and no more than 1.5 μm thick. On the Ferrograms, these particles are typically arranged in strings due to the magnetic field generated by the Ferrograph.

Two of the tests, MR4 and R4, yielded a second wear particle type. Typically, these particles were large bright flakes 20 to 60 μm in major dimension and <3 μm thick. An example of this particle type is shown in Fig. 12. They were located at random on the Ferrograms and were not normally aligned with the magnetic field. This behavior on the Ferrograms indicated that they were nonferrous and most likely aluminum. Heating the Ferrograms containing these particles to 330° C for 90 seconds caused the steel rubbing wear particles to change to a characteristic blue color. The blue color is caused by interference effects due to surface oxidation. The large flakes became bright silvery white confirming that they were aluminum. No doubt, there was a connection between the appearance of the large aluminum particles and the failure of the driving collar adhesive which occurred on tests MR4 and R4. This failure would cause the rotating drive

shaft to touch the aluminum housing thus producing aluminum wear particles. This particle type was not observed in any other oil samples.

Wear Regimes

A number of investigators have classified the various wear regimes that occur in sliding contacts. Reda, et al. (11) have identified six different wear regimes occurring at the interface between sliding steel surfaces. Each regime produces characteristic wear particles.

In regime 1 a full EHD film is normally present, wear rates are very low, and therefore few wear particles are observed. The wear particles that are observed are normally generated during start-up or shut-down where some metallic contact does occur. Typically, these particles are free metal of the normal rubbing wear type having major dimensions of less than 5 μm. Obviously, this regime corresponds to most tests of the present study where the Λ ratio is greater than 1.

Regime 2 refers to the normal boundary lubrication mode where there is a continuous generation of normal rubbing wear particles. These particles are free metal, less than 15 μm in major dimension and less than 1 μm thick. The rest of the tests from the present study fall into this regime where the Λ ratio is less than 1.

In regime 3, a breakdown of the boundary lubricant film occurs. The wear rate is high and the wear particles are free metal ranging in size from submicron to 150 μm. Regimes 4 and 5 are normally observed under unlubricated conditions and therefore do not really apply to this study. Regime 6 refers to the condition of catastropic surface failure resulting in free metal wear particles up to 1 mm. Obviously, regimes 3 and 6 were not observed in these studies.

Spectrometric Oil Analysis Results

A commonly used analytical method to determine the elemental concentrations of debris in a used oil is spectrometric analysis, commonly referred to as SOAP. An emission spectrograph was used to analyze each oil sample from this study. An unused oil sample was also tested as a blank. The blank contained small concentrations of a variety of different elements, but no iron or aluminum was detected. These elemental concentrations from the blank were then subtracted from all other readings. Results for the three elements (Fe, Al, and Cr) that could conceivably be related to the materials of the test rig appear in Table IV.

It is obvious from Table IV that most of the samples were barely within the limits of detection for the emission spectrograph. Little iron-containing wear debris was detected until the relatively high wear situation of the rough ball series was reached. However, even at the highest wear condition, R4, which had a composite Ferrogram density of 26.9, the spectrograph only detected 4 ppm of iron. This indicates that for detecting the iron-containing wear debris from these studies, the Ferrograph is more sensitive than the normal SOAP procedures.

The chromium present in the oil samples probably reflects the background variation in the blank. Chromium is present in the 52100 steel but it is at too low a concentration (1.5 percent) to be detected in these experiments. The aluminum in sample R4 is, no doubt, related to the driving collar failure. Its presence was discussed earlier. Sample S2 contained a large amount of extraneous debris which is reflected in the SOAP results as well as the Ferrogram densities.

Correlation of SOAP and Ferrogram Densities

After comparing the SOAP and Ferrograph results, there was a possi-

bility that the spectrograph might not be "seeing" all of the wear particles. This could be caused by a particle settling problem or a number of other factors. Therefore, in an attempt to correlate the results from the two techniques, the following assumptions were made. The average dimensions of the Ferrogram deposits were assumed to be: 50 mm long × 0.10 mm wide × 1.5 μm thick. Then for complete coverage (100 percent density reading), this corresponds to a particle volume of 7.5×10^{-3} mm^3. With a specific gravity of 8, the total mass of the deposit would be about 60 μg. Since approximately 3 grams of oil are passed over each Ferrogram, 60 μg of wear debris would represent about 20 ppm by weight. Multiplying the fractional optical densities of the rough ball series times 20, one obtains the following results: R1-0.4 ppm, R2-1 ppm, R3-4 ppm, and R4-5 ppm. Therefore, the SOAP results are consistent with the valves obtained with the Ferrograph.

Λ Variations as a Function of Test Time

In the normal operation of the EHD apparatus, the lubricant is circulated through a heat exchanger to maintain a constant bath temperature. During preliminary experiments, it was found that a great deal of extraneous debris was introduced into the oil from the recirculation system. This extraneous debris made it difficult to interpret the Ferrogram results. Therefore the heat exchanger was not utilized in these studies and no attempt was made to control the oil bath temperature. The bath temperatures were monitored during the course of each experiment and are tabulated in Table V.

Obviously, as the bath temperature rises there will be a corresponding decrease in viscosity and therefore in the film thickness and Λ. In addition, in the tests yielding appreciable wear (MR3 and 4, R2, 3, and 4),

there was a measurable decrease in ball surface roughness. This run-in effect has been noted by others (10). Taking these factors into account, all the Λ ratios at test conclusion were lower than the initial Λ value. However, only in tests S4, S5, and MR3, did the Λ ratios approach or cross over the transition value of 1. The final Λ ratios for S4, S5, and MR3 were 1, 1, and 0.5, respectively, and these values were reached only in the last few minutes of the test. Tests having initial Λ ratios greater than 3 yielded final Λ values greater than 1.5. All other tests had initial Λ values already below 1. Therefore, average Λ ratios (Λ_{avg}) for each test were used for the various correlations.

Ball Surface Temperatures

Ball surface temperatures were measured using the infrared technique previously described (6 and 7). Ball surface temperatures for the three test series appear in Fig. 13 as a function of maximum Hertz stress. Bath temperature was monitored during these tests and was maintained at about 40^{o} C except for the lowest load. Maximum temperatures of approximately 200^{o} C were observed in each test series at the highest load. At any given load, the ball surface temperatures were in the following order: rough > medium rough > smooth, as expected. A detailed analysis of these temperature measurements appears in reference 8.

A number of small blue metallic flakes were observed in the rough series Ferrograms while studying particle morphology. Only a few of these particles appeared in R1. However, as the load was increased, the occurrence of this particle type also increased and the maximum amount was observed in test R4. As previously mentioned this particle type is produced by short-term, high-temperature oxidation of the normal rubbing wear particles. In this case these blue particles were generated in situ by localized temperatures

probably much in excess of 330° C, but for very short times.

Friction Coefficients

Average friction coefficients for comparable tests measured at a steady state bath temperature of 40° C appear in Fig. 14. As one would expect, fairly constant values (0.061 to 0.062) were observed for all tests at average Λ ratios greater than 1.5 where a full EHD film existed. As asperity interactions increased as Λ_{avg} decreased below 1, the friction values also increased, as expected. No abrupt friction increases or transitions were observed which would have signaled a boundary film failure or a catastrophic failure mode. This agrees with the wear particle analysis previously discussed.

SUMMARY OF RESULTS

The Ferrograph was used to analyze oil samples from sliding EHD experiments. Chrome steel balls (AISI 52100) having surface roughnesses of 0.011, 0.076, and 0.38 μm Ra were slid against a sapphire flat. Test conditions included a sliding speed of 1.08 m/sec, a load range of 8.9 to 522 newtons, and a test duration of 25 minutes. Tests were conducted at room temperature. The major results were as follows:

1. The total amount of wear debris correlated well with calculated average Λ (film thickness to roughness) ratios. Much debris was observed at Λ values < 1, little debris at Λ's > 1.

2. The wear particles that were generated were metallic and almost exclusively of the normal rubbing wear type. No catastrophic failure modes were experienced.

3. Similar amounts of wear debris were observed in the different test series (different ball roughnesses) when compared at similar Λ ratios.

4. The Ferrograph was more sensitive in detecting the wear debris than was the commonly used emission spectrograph (SOAP analysis).

5. Maximum steady state ball surface temperatures of 200° C were observed with each test series at the highest load. Characteristic blue wear particles were observed with the rough ball series indicating much higher localized temperatures were generated.

Acknowledgement

The authors wish to thank Mr. Forest Handshaw of the Army Oil Analysis Laboratory at Fort Campbell, Kentucky for performing the spectrometric analysis on the oil samples.

REFERENCES

1. Seifert, W. W., and Westcott, V. C., "A Method for the Study of Wear Particles in Lubricating Oil," Wear, 21, 27-42 (1972).
2. Westcott, V. C., and Seifert, W. W., "Investigation of Iron Content of Lubricating Oils Using Ferrograph and Emission Spectrometer," Wear, 23, 239-249 (1973).
3. Scott, D., Seifert, W. W., and Westcott, V. C., "Ferrography - An Advanced Design Aid for the 80's," Wear, 34, 251-260 (1975).
4. Wedeven, L. D., "What is EHD?," Lubr. Eng., 31, 291-296 (1975).
5. Sanborn, D. M., and Winer, W. O., "Fluid Rheological Effects in Sliding Elastohydrodynamic Point Contacts with Transient Loading: I - Film Thickness," J. Lubr. Tech., 93, 262-271 (1971).
6. Turchina, V., Sanborn, D. M., and Winer, W. O., "Temperature Measurements in Sliding Elastohydrodynamic Point Contacts," J. Lubr. Tech., 96, 464-471 (1974).
7. Ausherman, V. K.; et al., "Infrared Temperature Mapping in Elastohydrodynamic Lubrication," J. Lubr. Tech., 98, 436-443 (1976).

8. Nagaraj, H. S., Sanborn, D. M., and Winer, W. O., "Effects of Load, Speed, and Surface Roughness on Sliding EHD Contact Temperatures," ASLE Preprint 76-LUB-23, Presented at the Joint ASME-ASLE Lubrication Conference, Boston, Mass., Oct. 1976.

9. Tallian, T. E., "On Competing Failure Modes in Rolling Contact," ASLE Trans., 10, 418-439 (1967).

10. Czichos, H.: Influence of Asperity Contact Conditions on Failure of Sliding Elastohydrodynamic Contacts, to be published in Wear Magazine.

11. Reda, A. A., Bowen, R., and Westcott, V. C., "Characteristics of Particles Generated at the Interface Between Sliding Steel Surfaces," Wear, 34, 261-273 (1975).

TABLE I. - EXPERIMENTAL TEST CONDITIONS

[Sliding speed for all tests was 1.08 m/sec.]

Test	Load, N		Maximum Hertz pressure, GN/m^2		Average Λ ratio, (Λ_{avg})
	Top contact	Bottom contact	Top contact	Bottom contact	
S1	8.9	3.6	0.52	0.39	22
S2	67	27	1.0	.76	10
S3	215	88	1.5	1.1	4.6
S4	307	125	1.7	1.3	1.8
S5	522	213	2.0	1.5	1.5
MR1	8.9	3.6	0.52	0.39	4.3
MR2	67	27	1.0	.76	2.0
MR3	215	88	1.5	1.1	.3
MR4	307	125	1.7	1.3	.2
R1	8.9	3.6	0.52	0.39	0.9
R2	67	27	1.0	.76	.4
R3	215	88	1.5	1.1	.1
R4	307	125	1.7	1.3	<0.1

TABLE II. - TEST FLUID PROPERTIES

Chemical type	Naphthenic mineral oil
Absolute viscosity, 38° C, N-sec/m^2 (cP)	2.18×10^{-2} (21.8)
Absolute viscosity, 99° C, N-sec/m^2 (cP)	3.2×10^{-3} (3.2)
Atmospheric pressure viscosity coefficient, $(N/m^2)^{-1}$	2.22×10^{-8}
Density, 38° C, G/ml	0.904
Density, 99° C, G/ml	0.866
Pour point, °C	-43
Flash point, °C	157
Fire point, °C	185
Molecular weight	305

TABLE III. - OPTICAL DENSITY OF FERROGRAMS AT VARIOUS FERROGRAM POSITIONS

Sample	Optical density at various positions on Ferrogram, percent							Composite density
	Entry	54	50	40	30	20	10	
S1	<1	<1	1.2	<1	<1	<1	<1	0.2
S2	15.3	4.4	1.0	1.9	1.3	1.8	<1	3.7
S3	4.2	4.3	<1	<1	<1	1.5	<1	1.4
S4	3.1	<1	<1	<1	<1	<1	<1	.4
S5	7.1	<1	<1	1.2	<1	<1	<1	1.2
MR1	1.6	1.8	1.8	<1	<1	4.1	2.6	1.7
MR2	3.7	1.6	1.2	<1	1.0	1.8	1.5	1.5
MR3	5.3	2.3	2.0	<1	<1	1.5	1.7	1.8
MR4	19.8	5.8	4.3	3.3	4.0	4.0	3.7	6.4
R1	7.1	2.0	1.0	1.4	<1	1.3	<1	1.8
R2	21.3	9.4	5.4	5.0	2.8	2.4	1.0	6.7
R3	36.9	24.6	19.6	14.0	10.4	11.7	14.0	18.7
R4	40.6	39.5	28.8	24.8	23.4	16.0	15.4	26.9

TABLE IV. - SPECTROGRAPHIC ANALYSIS OF OIL SAMPLES

Sample	Element concentration in parts per million		
	Fe	Al	Cr
S1	--	--	--
S2	1	2	1
S3	1	--	--
S4	1	--	--
S5	--	--	1
MR1	--	--	--
MR2	1	--	--
MR3	1	--	--
MR4	1	--	1
R1	--	--	--
R2	2	--	--
R3	3	--	--
R4	4	3	--

TABLE V. - OIL BATH TEMPERATURES (^{o}C)

AT VARIOUS TEST TIMES

Sample	Time, min									
	0	3	6	9	12	15	18	21	24	25
S1	25.5	26	26.3	26.6	26.9	27.2	27.5	27.7	27.8	27.8
S2	25.5	28.5	31.5	32.5	34	35.5	37	38	39.1	39.5
S3	24.5	33.5	38.5	43.7	48.2	52.3	57	58.9	62	63
S4	23.5	30.3	35.7	40	44	47	50.5	54	57.3	58.5
S5	26	32.5	36.9	40.2	43.2	46.1	48.7	51	53.5	54.3
MR1	23.5	23.9	24.4	24.8	25.1	25.4	25.7	25.9	26.1	26.2
MR2	22.3	26.7	29.1	31.1	32.9	34.4	35.9	37.4	38.6	39.0
MR3	23.8	35.8	43.3	50	56.7	61.5	64.6	68.1	72	73.2
MR4	25.2	41.7	55.5	62.8	70.5	76.5	82.3	85.4	[a]---	----
R1	25	25.6	26.3	26.8	27.2	27.6	28	28.4	28.7	28.8
R2	24.9	30.3	33.7	36.3	38.3	40.1	41.9	43.4	44.8	45.2
R3	25	42.7	52.3	59.3	65.3	71	75.6	80.3	84.2	85.5
R4	22.1	43.2	57.3	65.7	73.3	80	86.4	92.1	[a]---	----

[a]Tests terminated at 23 minutes due to failure of adhesive on driving collars.

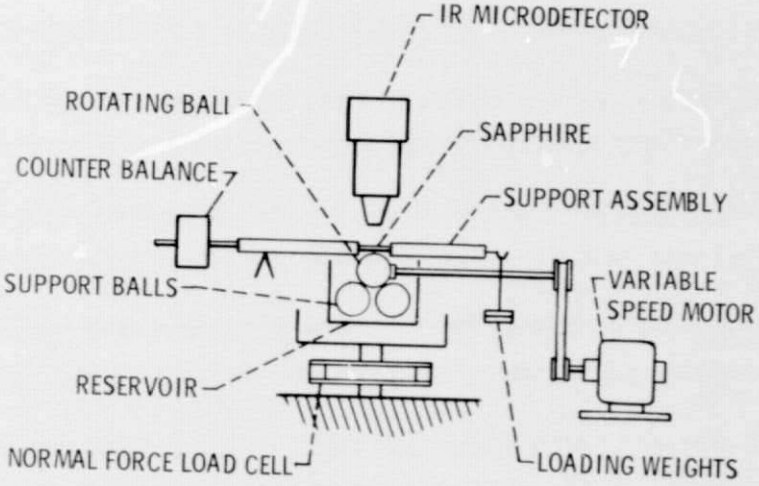

Figure 1. - Sliding EHD apparatus.

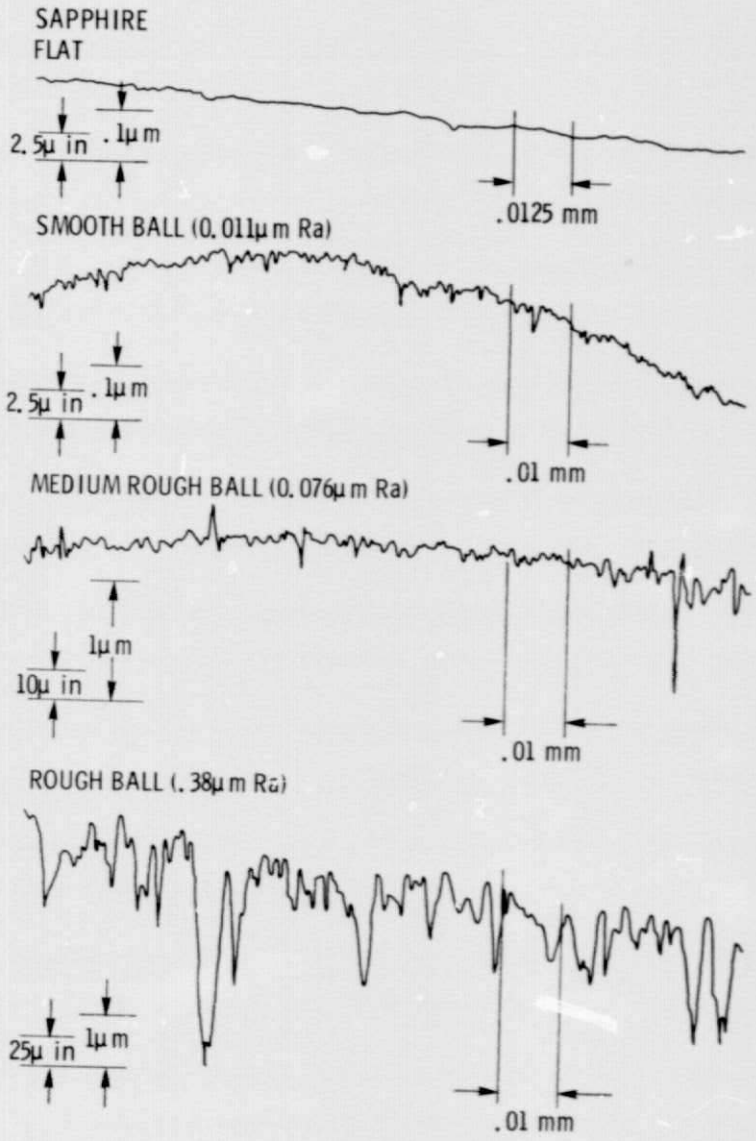

Figure 2. - Representative surface roughness profiles for the three test balls and sapphire flat.

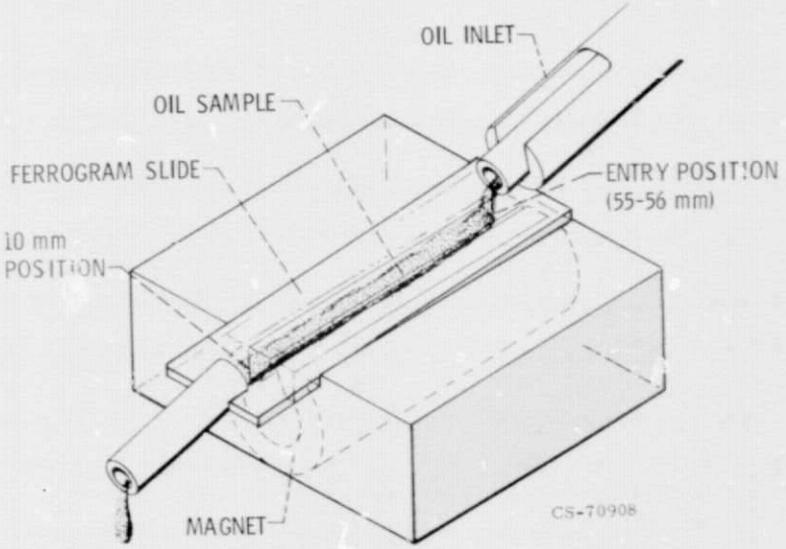

Figure 3. - Ferrograph analyzer.

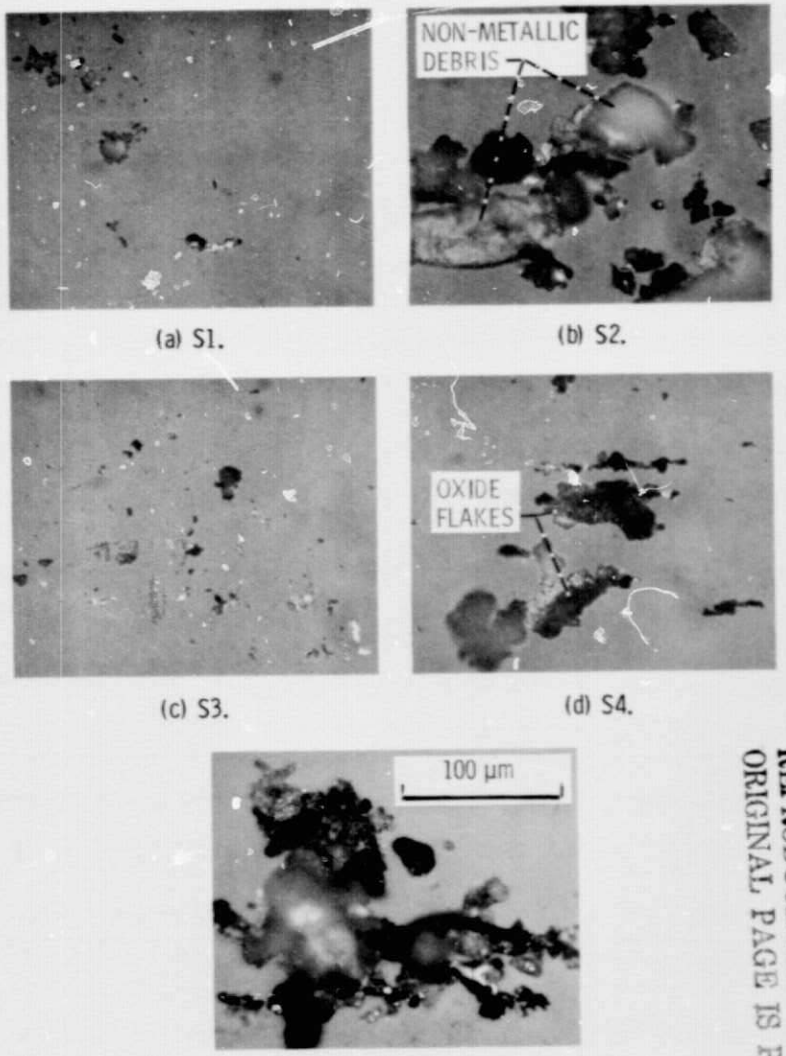

(a) S1. (b) S2.

(c) S3. (d) S4.

(e) S5.

Figure 4. - Ferrogram entry deposit for smooth series.

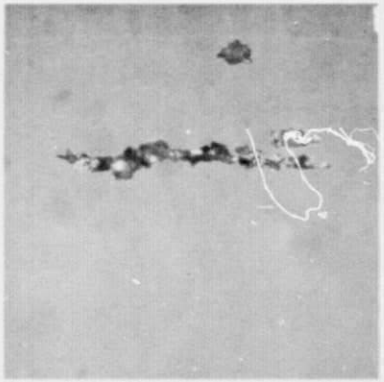

(a) MR1.

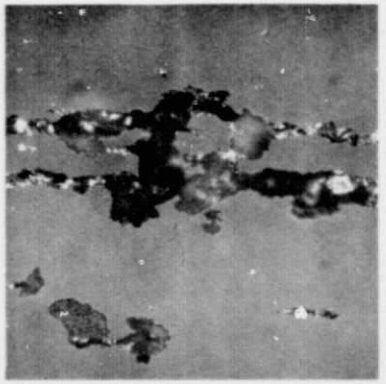

(b) MR2.

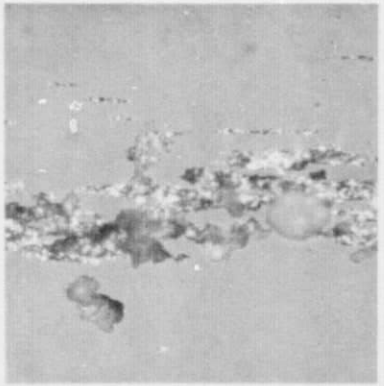

(c) MR3.

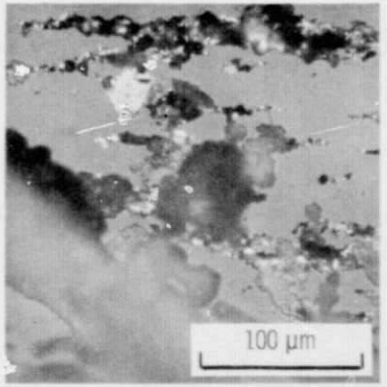

(d) MR4.

Figure 5. - Ferrogram entry deposit for medium rough series.

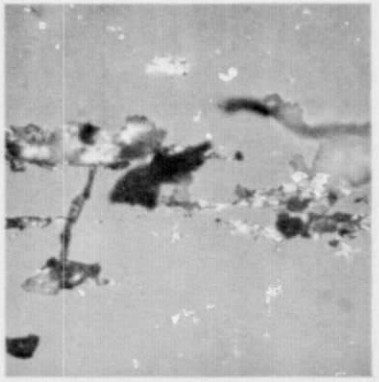

(a) R1.

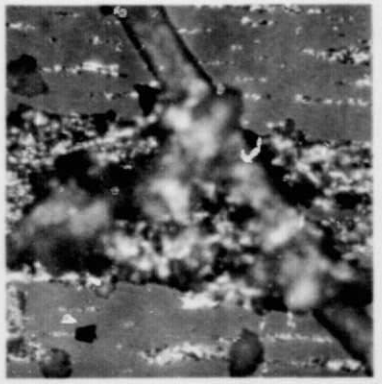

(b) R2.

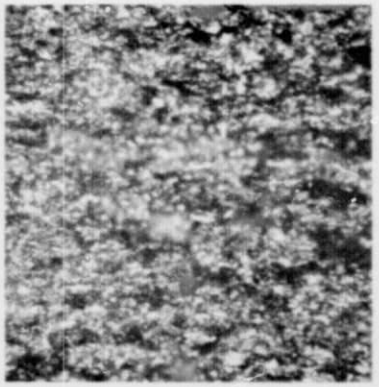

(c) R3.

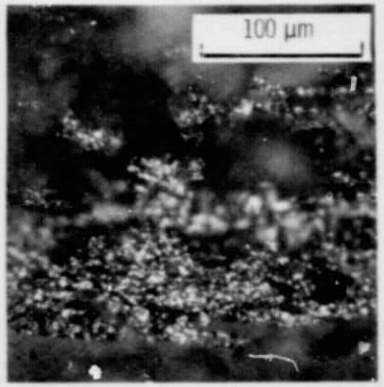

(d) R4.

Figure 6. - Ferrogram entry deposit for rough series.

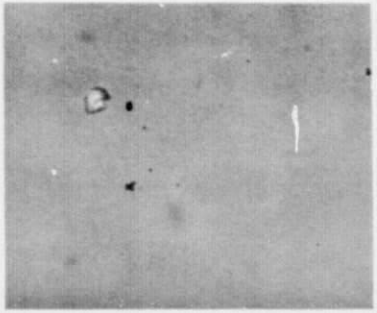

(a) S1.

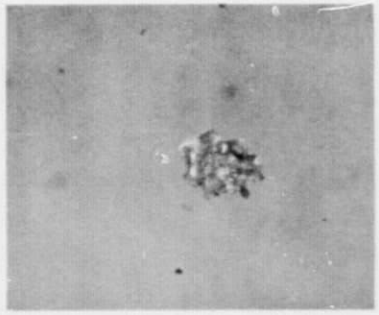

(b) S2.

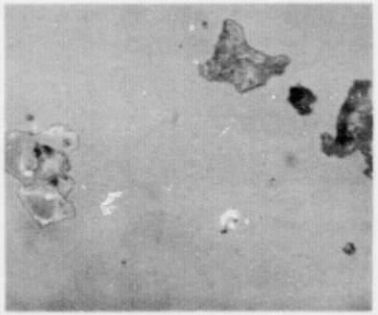

(c) S3.

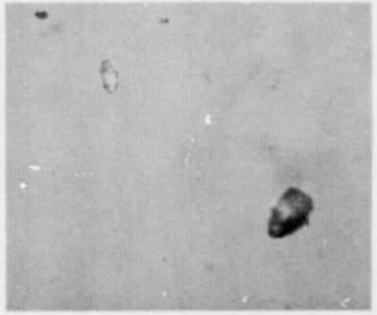

(d) S4.

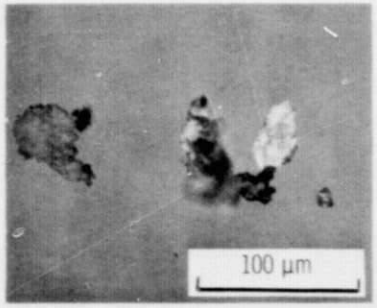

(e) S5.

Figure 7. - Ferrogram deposit at 54 mm for smooth series.

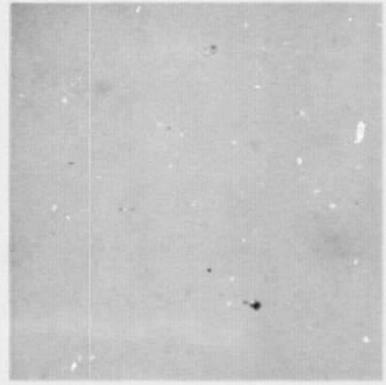

(a) MR1.

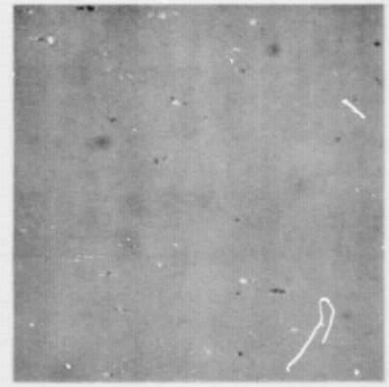

(b) MR2.

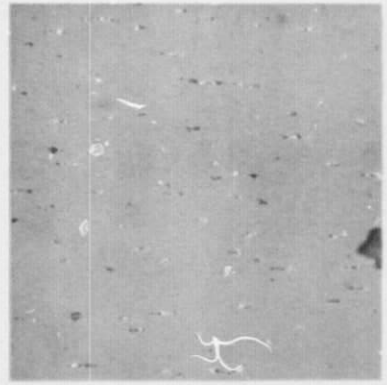

(c) MR3.

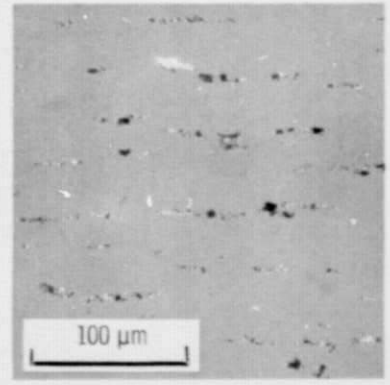

(d) MR4.

Figure 8. - Ferrogram deposit at 54 mm for medium rough series.

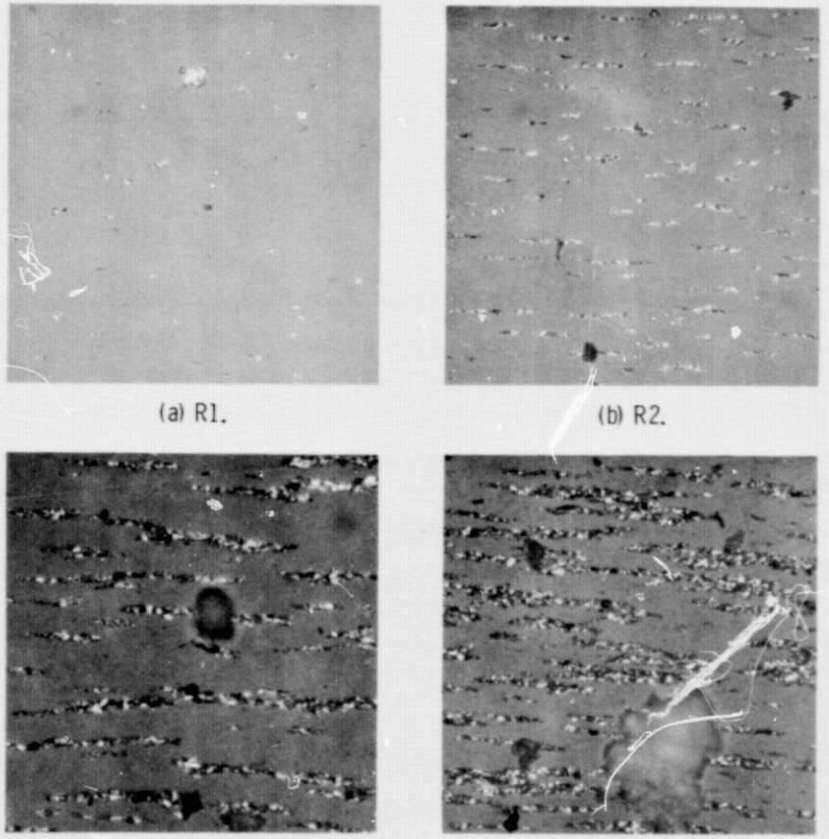

(a) R1. (b) R2.

(c) R3. (d) R4.

Figure 9. - Ferrogram deposit at 54 mm for rough series.

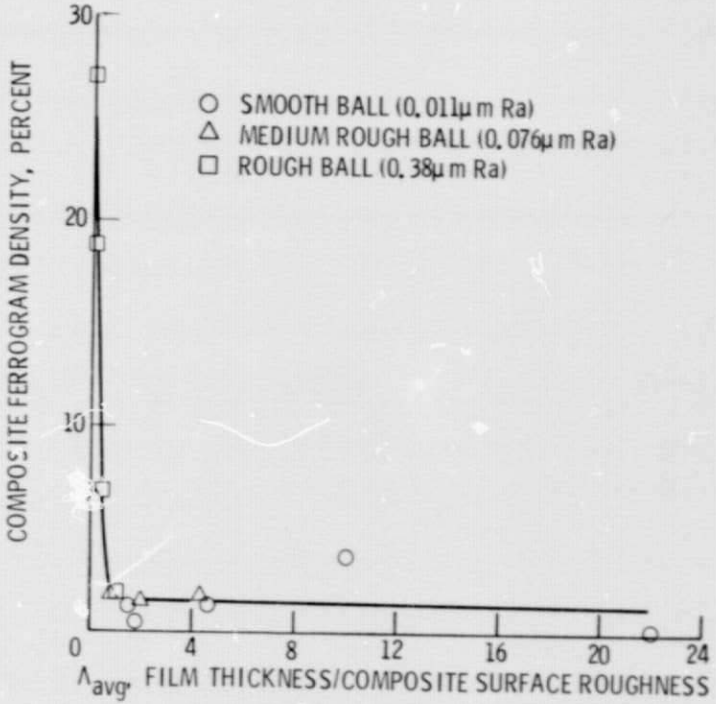

Figure 10. - Composite ferrogram density as a function of average Λ ratio (Λ_{avg}).

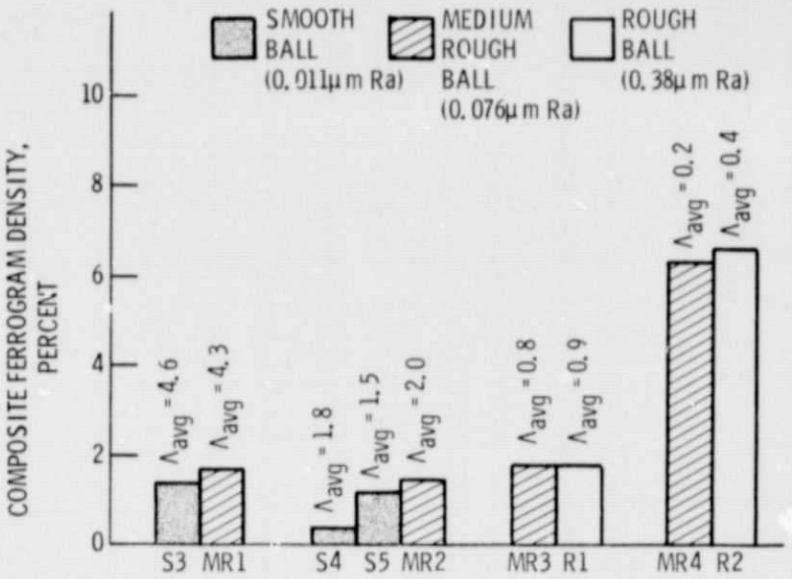

Figure 11. - Comparison of composite ferrogram densities at similar Λ_{avg} ratios.

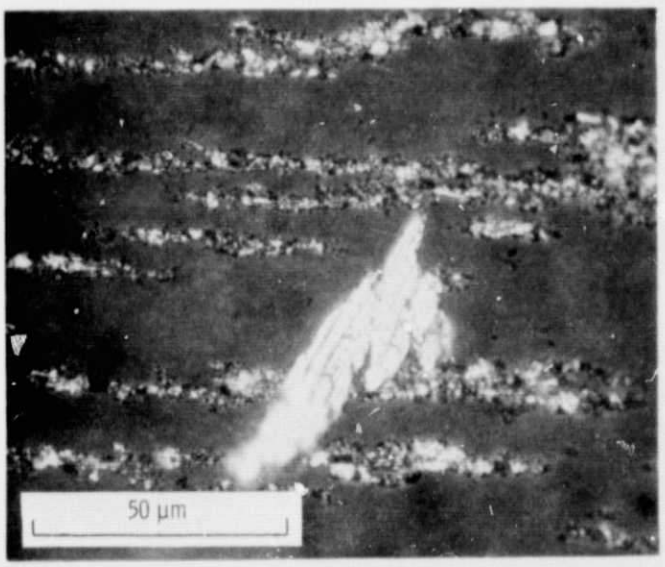

Figure 12. - Aluminum wear particle from test R4.

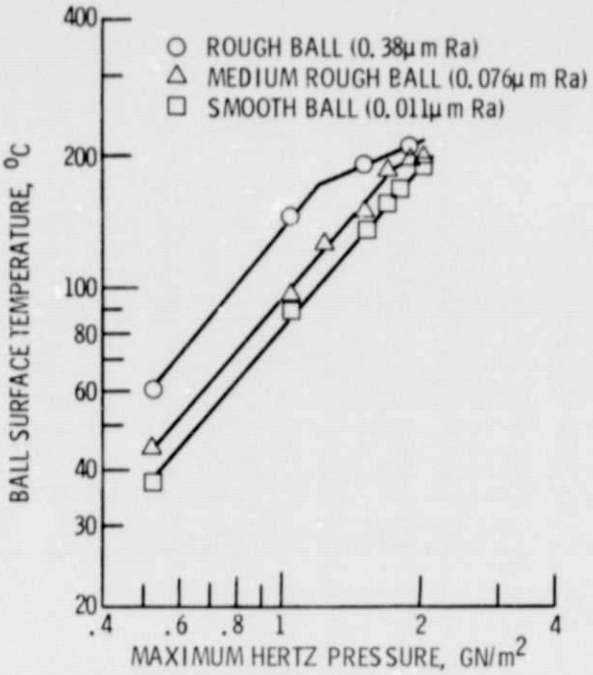

Figure 13. - Ball surface temperature as a function of maximum hertz pressure.

E-8925

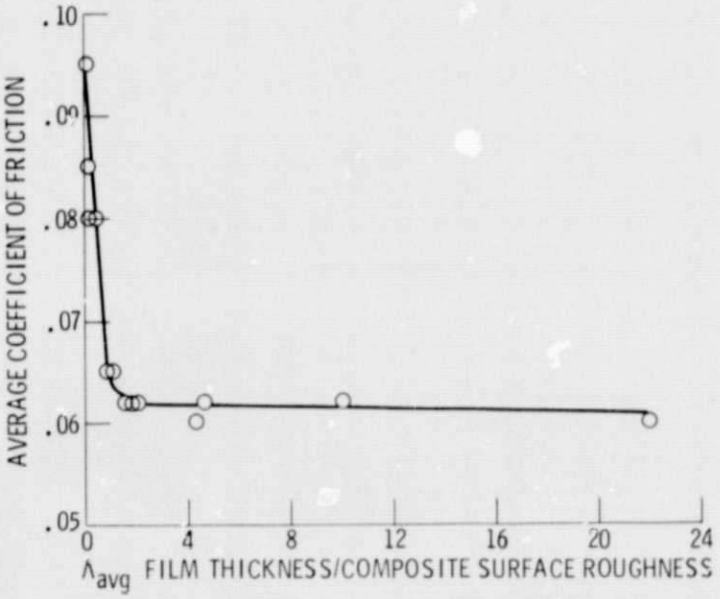

Figure 14. - Average coefficient of friction as a function as a function of average Λ ratio (Λ_{avg}).